


Article

Characteristics of Fine Particulate Matter (PM_{2.5})-Bound n-Alkanes and Polycyclic Aromatic Hydrocarbons (PAHs) in a Hong Kong Suburban Area

Yuan Gao ^{1,2}, Zhenhao Ling ^{3,*}, Zhuozhi Zhang ² and Shuncheng Lee ² 

¹ Instrumentation and Service Center for Science and Technology, Beijing Normal University, Zhuhai 519087, China; yuan.gao@bnu.edu.cn

² Department of Civil and Environmental Engineering, The Hong Kong Polytechnic University, Hong Kong 999077, China; zhuozhi.g.zhang@gmail.com (Z.Z.); shun-cheng.lee@polyu.edu.hk (S.L.)

³ School of Atmospheric Sciences, Sun Yat-sen University, Key Laboratory of Tropical Atmosphere-Ocean System, Ministry of Education, and Southern Marine Science and Engineering Guangdong Laboratory (Zhuhai), Zhuhai 519087, China

* Correspondence: lingzh3@mail.sysu.edu.cn

Abstract: PM_{2.5} samples were collected at Tung Chung (TC), Hong Kong, during four nonconsecutive months in 2011/2012 to determine the concentrations, seasonal variations, and potential sources of polycyclic aromatic hydrocarbons (PAHs) and n-alkanes (*n*-C₁₅-*n*-C₃₅). Samples were analyzed using the thermal desorption gas chromatography/mass spectrometry (TD-GC/MS) method. The concentrations of particulate PAHs ranged from 1.26–13.93 ng/m³ with a mean value of 2.57 ng/m³, dominated by 4-ring species. Phenanthrene (Phe) and fluoranthene (Flu) were the two most abundant species, accounting for 13% and 18%, respectively. The dominant sources of PAHs were coal and biomass burning. The inhalation cancer risk value in our study exceeded 1×10^{-6} but was below 1×10^{-4} , implying that the inhalation cancer risk of PAHs at the TC site is acceptable. The average concentration of n-alkanes was 103.21 ng/m³ (ranging from 38.58 to 191.44 ng/m³), and C₂₅ was the most abundant species. Both PAHs and n-alkanes showed higher concentrations in autumn and winter whilst these values were lowest in summer. The carbon preference index (CPI) and percent contribution of wax n-alkanes showed that biogenic sources were the major sources. The annual average contributions of higher plant wax to n-alkanes at TC were over 40%.

Keywords: fine particulate matter (PM_{2.5}); polycyclic aromatic hydrocarbons (PAHs); n-alkanes; suburban area



Citation: Gao, Y.; Ling, Z.; Zhang, Z.; Lee, S. Characteristics of Fine Particulate Matter (PM_{2.5})-Bound n-Alkanes and Polycyclic Aromatic Hydrocarbons (PAHs) in a Hong Kong Suburban Area. *Atmosphere* **2022**, *13*, 980. <https://doi.org/10.3390/atmos13060980>

Academic Editor: Célia Alves

Received: 25 May 2022

Accepted: 14 June 2022

Published: 17 June 2022

Publisher's Note: MDPI stays neutral with regard to jurisdictional claims in published maps and institutional affiliations.



Copyright: © 2022 by the authors. Licensee MDPI, Basel, Switzerland. This article is an open access article distributed under the terms and conditions of the Creative Commons Attribution (CC BY) license (<https://creativecommons.org/licenses/by/4.0/>).

1. Introduction

Organic aerosols are a major component of PM_{2.5} and have a direct impact on the environment and human health due to their abundance in the ambient environment and complex physical and chemical properties. In midlatitude continental areas, the contribution of organic aerosols to PM_{2.5} ranged from 20% to 50% [1–4]; in China, organic aerosols comprise ~35% on average [5]. Organic aerosols can be emitted from both anthropogenic activities, e.g., incomplete combustion of fossil fuel, and natural sources, e.g., volcanic eruptions. Although many studies have investigated the importance of organic aerosols, the levels, formation mechanisms, and chemical characteristics of organic species are different from microenvironments; thereby, to obtain a holistic understanding, further investigation of organic aerosol is needed.

In the past century, only a small fraction of organic aerosols has been identified at the molecular level [6]. Polycyclic aromatic hydrocarbons (PAHs) and n-alkanes are the two important components of organic aerosols. Both PAHs and n-alkanes can be emitted to the environment through anthropogenic activities, e.g., incomplete combustion

of fossil fuel; petroleum residues; and natural sources, e.g., wildfire [7,8]. Biogenic sources, including particles shed from leaf epicuticular wax and suspensions of pollen, fungi, bacteria, algae, and higher plant waxes, play important roles in *n*-alkane emissions to the environment [9–11].

The two pollutants have recently received much attention due to their negative impacts on humans; for example, *n*-alkanes can damage skin and engender skin cancer. Many PAH species are known to be carcinogenic, mutagenic, or teratogenic. For example, benzo(a)pyrene, benzo(b)fluoranthene, benzo(k)fluoranthene, and indeno(1,2,3-cd)pyrene are known for their carcinogenic properties and can bioaccumulate in the environment [7,12]. Their presence and characteristics have been widely studied worldwide and in many Chinese megacities, such as Beijing, Nanjing, Guangzhou, etc. [13–15]. Different areas showed varied dominant sources, for example, 25% of *n*-alkanes were from plant wax, and 37% of PAHs were from biomass burning in Lulang [16] while in Guangzhou, the significant pollution source of PAHs and *n*-alkanes was from coal combustion [13]. Previous Hong Kong studies have mainly focused on identifying the characteristics and sources of PAHs and *n*-alkanes in urban and industrial areas. However, the influential features of these two pollutants in different microenvironments can vary. For example, in urban areas, the major contributor of PAHs and *n*-alkanes is traffic emission, but in industrial areas, the dominant source of the two pollutants is stationary emissions [17,18].

Tung Chung (TC) is a new town in Hong Kong, which was developed to serve as a supporting community for one of the world's busiest passenger airports (Hong Kong Chep Lap Kok airport), including government public facilities, commercial centers, office blocks, and hotels. In 2016, TC had over 86,000 inhabitants (2016 census) and the development of TC areas is still ongoing to support the growing population. This area is surrounded by many large country parks with many natural resources and located in the centerline of the Pearl River Delta (PRD) region, facing Macau and mainland China. Therefore, this sampling area becomes a speculated microenvironment with mixing with complex potential sources of PAHs and *n*-alkanes. However, limited PAH- and *n*-alkane-related studies have been conducted here. To fill the gap in the study of PAHs and *n*-alkanes in the area, we conducted 4 months of sampling from 2011–2012 to understand the abundance, seasonal variation, and possible sources of particle-associated PAHs and *n*-alkanes.

2. Materials and Methods

2.1. Sampling Site and Sample Collection

All samples were collected at the TC site (22.17° N, 113.56° E), which is located on the northern coast of Lantau Island and is southwest of Hong Kong (Figure 1), surrounded by three mountains. The sampling was conducted in four nonconsecutive months, which were August (2011), November (2011), February (2012), and May (2012), representing summer, autumn, winter, and spring, respectively. The sampling instruments were placed on the rooftop of a three-story building, which was established by Hong Kong Environmental Protection Department (HKEPD). Detailed information of the sampling site was illustrated in an earlier study [19].

Twenty-four-hour integrated PM_{2.5} samples (from 10:00 a.m. to 10:00 a.m. the next day local standard time) were collected by a high-volume sampler manufactured by Graseby Andersen (Model Tisch Environmental Inc., Village of Cleves, OH, USA) with a flow rate of 1.13–1.41 m³/min. A total of seven PM_{2.5} samples were collected in each season. Table S1 lists the sampling dates and daily meteorological conditions. Whatman quartz microfiber filters (20.3 cm × 25.4 cm) were used. Before sampling, all quartz-fiber filters were preheated at 900 °C for 3 h to minimize organic artifacts [20]. Four field blank filters were collected during the four sampling periods. After sampling, the samples were properly stored in a freezer at −20 °C to minimize the loss of volatiles.

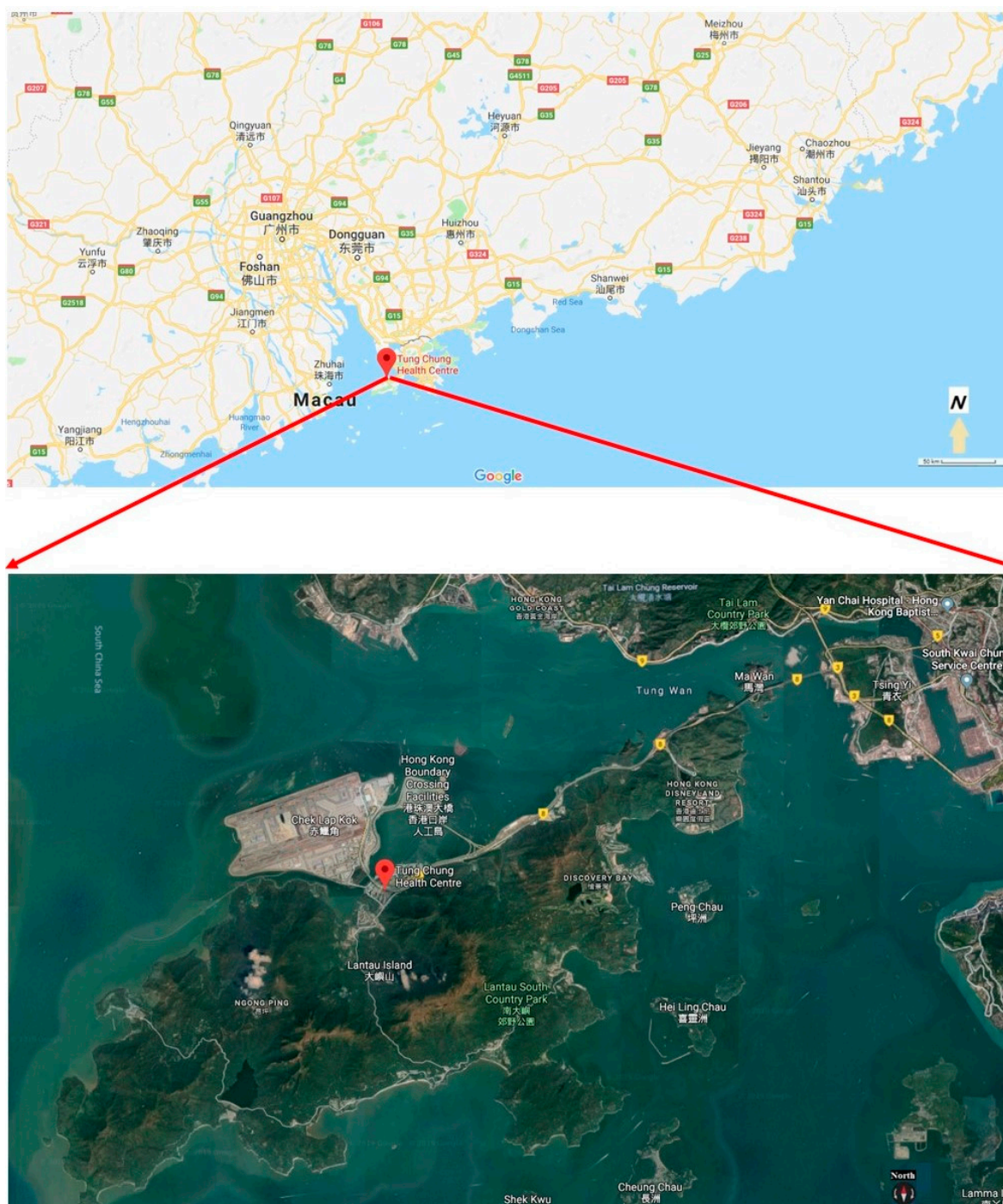


Figure 1. Location of the sampling site. Source: from Google map.

2.2. Chemical Analysis

After sampling, the filters were conditioned and weighed to determine the mass concentration of the loaded particles. The filters were cut into small portions and analyzed at the Institute of Earth Environment, Chinese Academy of Science (Xi’an) using the thermal desorption-gas chromatography/mass spectrometry (TD-GC-MS) method with the use of an Agilent 6890A/5975C system. The filter was cut into smaller strips and inserted into a TD tube with wool plugged in both ends of the tube. The HP-5ms capillary column (5% diphenyl/95% dimethylsiloxane; 30 m long × 0.25 mm I.D. (Internal Diameter) × 0.25 μm film thick; J&K Scientific, Folsom, CA, USA) was used to separate the compounds. The carrier gas was ultra-high-purity (99.999%) helium (He) at a constant flow of 1.0 cm³/min. All

the organic compounds desorbed from the filter below 275 °C. The details of this analysis method were described by Ho et al. [21]. A total of 20 PAHs, including acenaphthylene (AC), acenaphthene (ACE), fluorene (Flo), phenanthrene (Phe), anthracene (Ant), fluoranthene (Flu), pyrene (Pyr), benzo(a)anthracene (BaA), chrysene (Chr), benzo(b)fluoranthene (BbF), benzo(k)fluoranthene (BkF), benzo(a)fluoranthene (BaF), benzo(e)pyrene (BeP), benzo(a)pyrene (BaP), perylene (Per), indeno(1,2,3-cd)pyrene (IcdP), dibenzo(a,h)anthracene (DahA), benzo(ghi)perylene (BghiP), coronene (Cor), dibenzo(a,e)pyrene (DaeP), and 21 *n*-alkanes (i.e., from C₁₅–C₃₅), were determined.

For ion analysis, half of the quartz-fiber filters were extracted with 10 mL of ultrapure water (specific resistance ≥ 18.1 M Ω ·cm, Millipore). The extraction solution was analyzed by ion chromatography (ICS3000, DIONEX, Sunnyvale, CA, USA) for water-soluble ions, including chloride (Cl⁻), nitrate (NO₃⁻), sulfate (SO₄²⁻), sodium (Na⁺), potassium (K⁺), calcium (Ca²⁺), and ammonium (NH₄⁺). The concentration data is shown in the Supplementary Materials Table S2.

Other gaseous measurements included CO, NO_x, and O₃, which were measured with a CO analyzer (TEI, Model 48C), chemiluminescence NO_x analyzer (TEI, Model 42i with blue light converter), and UV photometric O₃ analyzer (Teledyne, API 400), respectively. Meteorological parameters (wind profile, temperature, and relative humidity) were also monitored with an RH/T probe and wind monitor (Gill, UK) at the sampling site. The sampling interval of the gaseous species and meteorological parameters was 1 min. Span and zero calibration of the gas analyzers was carried out every week. The daily average data is shown in the Supplementary Materials Table S2.

2.3. Risk Assessment

The BaP equivalent concentration (BaP_{eq}) was used to assess the health risk of PAHs; the equation of BaP_{eq} is shown in Equation (1):

$$\text{BaP}_{\text{eq}} = \sum C_i \times \text{TEF}_i \quad (1)$$

where C_i refers to the mass concentration of specific PAHs components (Phe, Ant, Flu, Pyr, BaA, Chr, BbF, BkF, BeP, BaP, Per, IcdP, BghiP, and DahA). Based on Nisbet and LaGoy [22], the TEF_{*i*} values of the specific PAHs components are Phe (0.001), Ant (0.01), Flu (0.001), Pyr (0.001), BaA (0.01), Chr (0.01), BbF (0.1), BkF (0.1), BeP (0.01), BaP (1), Per (0.001), IcdP (0.1), BghiP (0.01), and DahA (5).

The inhalation cancer risk (ILCR) was used to estimate the cancer risk from PAH exposure, which was calculated by multiplying BaP_{eq} and inhalation unit risk (UR_{BaP}). The UR_{BaP} value was the maximum theoretical increased probability of lung cancer that was caused by continuing exposure to atmospheric BaP (1 ng/m³) in a 70-year life time. According to WHO [23], the UR_{BaP} value is 8.7×10^{-5} . The ILCR was calculated using Equation (2):

$$\text{ILCR} = \sum \text{BaP}_{\text{eq}} \times \text{UR}_{\text{eq}} \quad (2)$$

3. Results and Discussion

3.1. PAH (Polycyclic Aromatic Hydrocarbon) Concentrations, Seasonal Variations, and Potential Health Risks

The sum of the PAH concentrations (19 species) ranged from 1.26–13.93 ng/m³, with an average concentration of 2.57 ± 2.53 ng/m³, during the whole sampling period in the Hong Kong suburban area (Table 1). The reported value was lower than those measured in the Hong Kong, Guangzhou, Xiamen, and Sanya urban areas, which were 10.72, 23.70, 10.10 and 9.90 ng/m³, respectively [17,24–27]. The values measured in a Hong Kong rural area (1.90 ng/m³), Korean rural area (2.24 ng/m³), and Finland suburban area (3.27 ng/m³) were comparable to the values measured in this study [28–30]. The PAH value has been measured in Hong Kong since 1994, and its concentration in a rural area was 4.16 ng/m³ [31]. After 10 years, the PAH concentration was 1.90 ng/m³ at the same site [28]. In the past 15 years,

a 2–3-fold reduction in the PAH value was also observed in the Hong Kong urban area, from 10.72 ng/m³ in 2000–2001 [17] to 4.59 and 3.46 ng/m³ in 2011–2012 [32] and 2014 [33], respectively. This may be attributed to the reduction in local on-road traffic emissions. In addition, from a study by Liao et al. [34], for PAHs, especially BaP, the reduction rate was approximately 0.013 ng/m³ per year, which was due to declining emissions from vehicular exhaust and biomass/coal combustion. By determining the abundance of 20 PAHs in PM_{2.5} samples, Phe and Flu were found to be the dominant species in the four seasons (Figure 2). The average concentrations of Phe and Flu were 0.27 and 0.38 ng/m³, respectively. The annual percent contributions of the two most abundant compounds relative to ΣPAHs were 13% (Phe) and 18% (Flu), which collectively accounted for approximately 31%. The authors of [31] reported a similar situation in a rural area of Hong Kong (Hok Tsui), and they attributed this to some of the previously deposited Phe and Flu being revolatilized and re-emitted into the atmosphere. Notably, one summer pollution episode was observed during sampling. The average PAH concentration was up to 13.93 ng/m³, and the abundant species were Chr, BbF, BkF, and BeP, with values of 1.83, 2.74, 1.64, and 1.77 ng/m³, respectively, and accounted for approximately 60% of the ΣPAH concentration. Many studies have pointed to stationary emissions if there is a high factor loading of Chr and BbF [7,8,35].

Table 1. Mass concentration of PAH components (ng/m³) in PM_{2.5} at TC, Hong Kong.

		Summer		Autumn		Winter		Spring		Annual	
		Average	S.D.	Average	S.D.	Average	S.D.	Average	S.D.	Average	S.D.
3-ring	AC	0.05	0.03	0.06	0.02	0.10	0.05	0.07	0.02	0.07	0.03
3-ring	ACE	0.01	0.01	0.01	0.01	0.01	0.01	0.01	0.01	0.01	0.01
3-ring	Flo	0.04	0.02	0.05	0.01	0.06	0.02	0.04	0.01	0.05	0.02
3-ring	Phe	0.27	0.11	0.21	0.08	0.39	0.14	0.23	0.05	0.27	0.12
3-ring	Ant	0.12	0.02	0.16	0.07	0.17	0.04	0.16	0.04	0.16	0.05
4-ring	Flu	0.37	0.14	0.29	0.13	0.56	0.24	0.31	0.07	0.38	0.18
4-ring	Pyr	0.18	0.08	0.16	0.06	0.29	0.13	0.15	0.03	0.20	0.10
4-ring	BaA	0.03	0.02	0.04	0.02	0.06	0.02	0.03	0.00	0.04	0.02
4-ring	Chr	0.15	0.07	0.21	0.13	0.25	0.09	0.17	0.02	0.20	0.10
5-ring	BbF	0.09	0.03	0.18	0.09	0.17	0.06	0.09	0.02	0.14	0.08
5-ring	BkF	0.09	0.04	0.17	0.12	0.19	0.05	0.09	0.03	0.14	0.09
5-ring	BaF	0.03	0.01	0.03	0.03	0.03	0.02	0.02	0.01	0.03	0.02
5-ring	BeP	0.07	0.02	0.21	0.15	0.19	0.07	0.09	0.03	0.15	0.13
5-ring	BaP	0.02	0.01	0.05	0.02	0.12	0.15	0.03	0.01	0.05	0.08
5-ring	Per	0.03	0.01	0.03	0.01	0.04	0.03	0.03	0.01	0.03	0.01
6-ring	IcdP	0.02	0.02	0.07	0.04	0.05	0.02	0.03	0.02	0.05	0.03
5-ring	DahA	0.01	0.00	0.02	0.01	0.01	0.00	0.01	0.00	0.01	0.01
6-ring	BghiP	0.04	0.01	0.13	0.11	0.09	0.04	0.05	0.03	0.08	0.07
7-ring	Cor	nd	nd	0.07	0.02	0.11	0.00	0.08	0.03	0.08	0.02
ΣPAH		1.62	0.64	2.15	1.13	2.90	1.19	1.67	0.43	2.57	2.53

As shown in Figure 3, the mean PAH concentrations observed in the autumn (2.15 ng/m³) and winter (2.90 ng/m³) are higher than those in summer (1.62 ng/m³) and spring (1.67 ng/m³). In summer and spring, stronger thermal circulation and deeper mixing heights result in excellent dilution and dispersion of pollutants, effectively causing the diffusion and dilution of PAHs [36]. Therefore, relatively low PAH values were observed. In autumn and winter, the predominant wind brings relatively high concentrations of particles matter pollutants from mainland China [36]. From Table S1, relatively high PAHs were observed when the predominant wind was from north, northeast, and northwest. A more detailed picture of the seasonal variations in the 19 PAH species is shown in Figure 3. The targeted PAHs can be grouped into three categories: 3-ring compounds, 4-ring compounds, and 5,6,7-ring compounds. The dominant PAHs in our study were 4-ring compounds in summer, winter, and spring, accounting for 44%, 40%, and 40%, respectively. The contri-

bution of 3-ring PAHs ranged from 22% to 31% during the four seasons, with the highest contribution in summer. The major contributor in autumn was observed as the 5,6,7-ring compounds (45%).

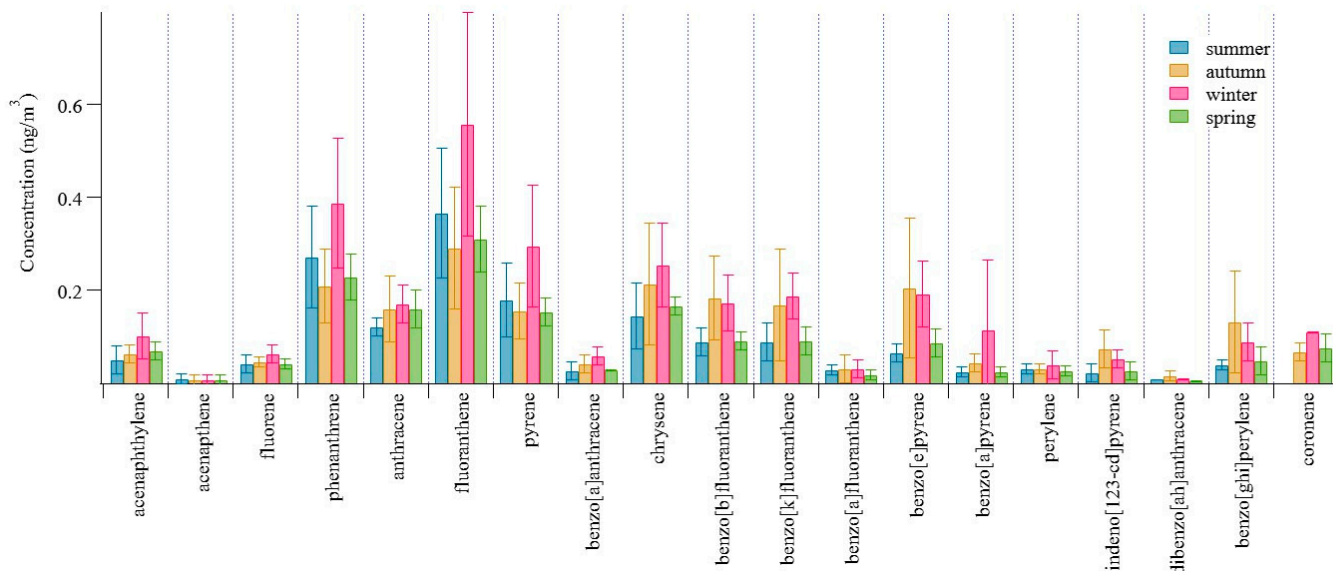


Figure 2. The abundance of detected PAH components in various seasons (unit: ng/m^3 ; blue: summer, yellow: autumn, red: winter, green: spring).

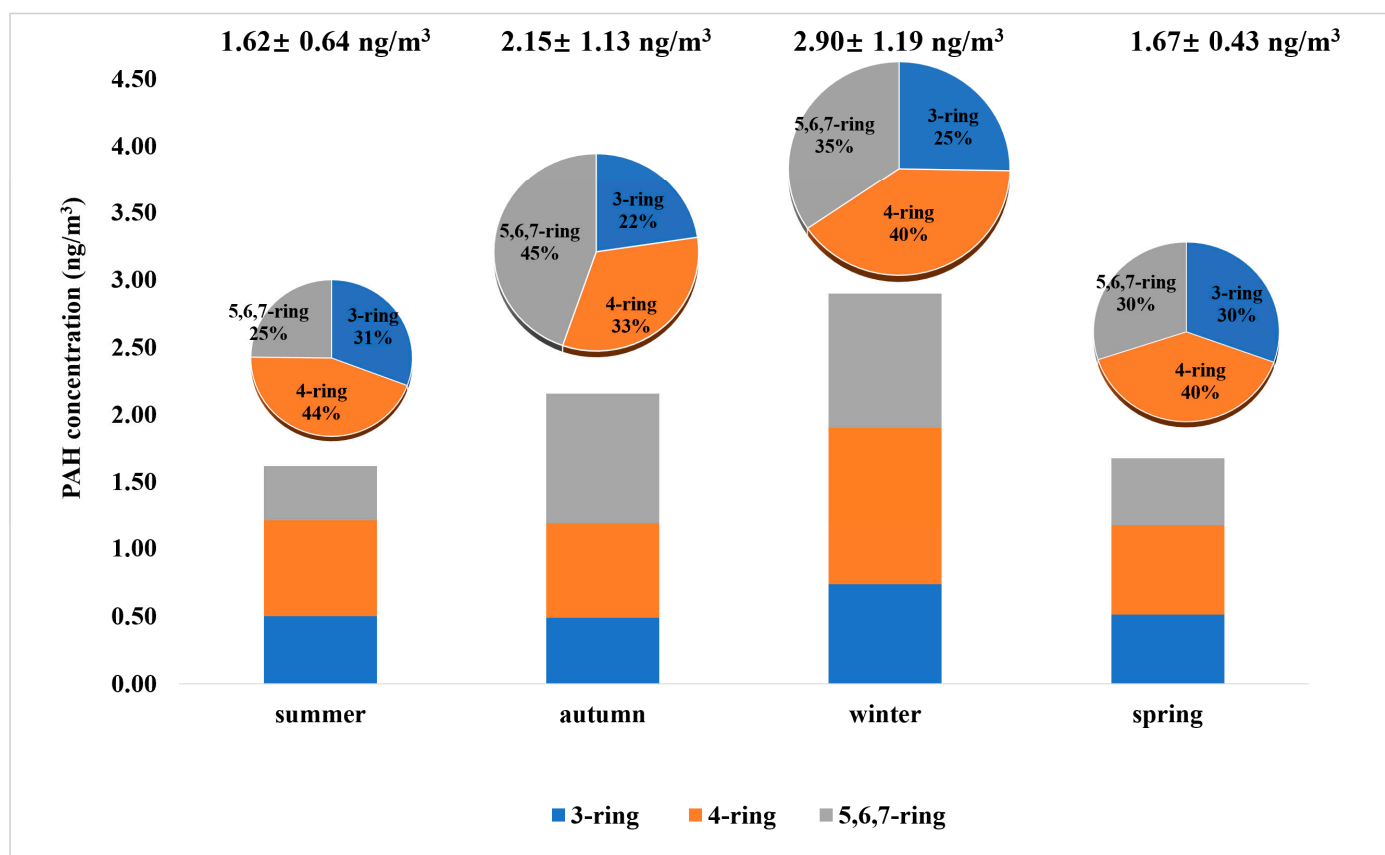


Figure 3. Relative concentrations of the 3-, 4-, and 5,6,7-ring groups in different seasons (unit: ng/m^3 ; blue: 3-ring PAH species, orange: 4-ring PAH species, grey: 5,6,7-ring PAH species).

In this study, the observed BaP concentration was 0.024–0.115 ng/m³, which is below the value of the Chinese standard (2.5 ng/m³) and EU standard (1 ng/m³). Based on Equation (1), BaP_{eq} was calculated, and its mean value was 0.06 ± 0.02, 0.16 ± 0.09, 0.20 ± 0.14, and 0.08 ± 0.03 ng/m³ in summer, autumn, winter, and spring, respectively. The value is lower than those reported of many urban areas, such as 0.77 ng/m³ in Xiamen (China), 4.10 ng/m³ in Guangzhou (China), 1.91 ng/m³ in Fuji (Japan), 0.99 ng/m³ in Birmingham (UK), and a rural area in Hong Kong, China (0.31 ng/m³) [25,26,28,37,38]. The ILCR value (via Equation (2)) in our study ranged from 5.4 × 10⁻⁶ to 1.7 × 10⁻⁵, with a mean value of 1.1 × 10⁻⁵. According to the US-EPA and Liu et al. [39], the reported ILCR values lower than 1 × 10⁻⁶ and 1 × 10⁻⁴ and higher than 1 × 10⁻⁴ can be defined as a negligible, acceptable, and serious cancer risk level, respectively. Therefore, the ILCR value in our study exceeded 1 × 10⁻⁶ but was below 1 × 10⁻⁴, indicating that the inhalation cancer risk of PAH in TC, HK is acceptable.

3.2. *n*-Alkanes Concentrations and Seasonal Variations

A set of 21 *n*-alkanes (C₁₅–C₃₅) were investigated in this study, and the average concentrations of these compounds are presented in Table 2. C₂₅ was the most abundant species of the *n*-alkane homologs, with a value of 12.48 ng/m³. C₂₉ and C₂₃ also exhibited a high abundance, with concentrations of 12.27 and 12.20 ng/m³, respectively. Most *n*-alkane species were below 10 ng/m³. The sum of the measured *n*-alkane concentrations ranged from 38.58 to 191.44 ng/m³, with a mean value of 103.21 ng/m³ for the entire study. In comparison, the average *n*-alkane concentration was much lower than the concentrations observed in other urban areas of China: 225 ng/m³ in Nanjing, 184 ng/m³ in Ningbo, and 163 ng/m³ in Beijing [14,15,40]. Relatively low values were observed in a Hong Kong rural area (23.5 ng/m³) [31], Lulang in Tibet (1.25 ng/m³) [16], and Sanya (5.7 ng/m³) [27]. The observed *n*-alkane values at TC were comparable with those reported for some major cities in China, such as Shanghai (93.7 ng/m³) [40] and Guangzhou (102 ng/m³) [13].

Table 2. Mass concentration of *n*-alkane (ng/m³) components in PM_{2.5} at TC, HK.

	Summer		Autumn		Winter		Spring		Annual	
	Average	S.D.	Average	S.D.	Average	S.D.	Average	S.D.	Average	S.D.
<i>n</i> -pentadecane (C ₁₅)	0.43	0.07	0.47	0.22	0.52	0.26	0.49	0.15	0.48	0.18
<i>n</i> -hexadecane (C ₁₆)	0.49	0.11	0.76	0.41	0.70	0.24	0.80	0.31	0.70	0.31
<i>n</i> -heptadecane (C ₁₇)	0.67	0.12	0.74	0.23	0.85	0.25	1.13	0.80	0.85	0.45
<i>n</i> -octadecane (C ₁₈)	0.92	0.13	1.40	0.18	1.34	0.61	1.32	0.46	1.27	0.41
<i>n</i> -nonadecane (C ₁₉)	1.11	0.38	1.67	0.74	1.74	0.52	1.50	0.85	1.53	0.66
<i>n</i> -icosane (C ₂₀)	0.90	0.37	1.09	0.47	0.98	0.47	1.38	0.64	1.10	0.50
<i>n</i> -heneicosane (C ₂₁)	1.75	1.30	2.09	0.92	2.03	1.58	3.26	2.12	2.30	1.54
<i>n</i> -docosane (C ₂₂)	2.85	2.17	4.04	2.24	3.24	2.81	6.21	4.21	4.13	3.06
<i>n</i> -tricosane (C ₂₃)	7.23	8.08	12.47	8.55	10.45	8.86	17.77	10.85	12.20	9.35
<i>n</i> -tetracosane (C ₂₄)	5.36	4.69	11.22	5.06	10.99	6.52	11.37	4.98	9.98	5.57
<i>n</i> -pentacosane (C ₂₅)	7.55	4.67	14.75	8.28	11.93	4.79	14.48	4.78	12.48	6.29
<i>n</i> -hexacosane (C ₂₆)	4.87	2.95	7.82	4.77	9.47	5.37	6.78	4.05	7.36	4.47
<i>n</i> -heptacosane (C ₂₇)	8.34	3.78	12.24	5.79	12.07	4.65	10.70	4.22	11.00	4.70
<i>n</i> -octacosane (C ₂₈)	4.15	2.26	6.10	3.30	6.87	3.44	4.85	2.16	5.57	2.90
<i>n</i> -nonacosane (C ₂₉)	10.36	3.94	12.17	3.24	13.04	3.21	13.20	5.22	12.27	3.85
<i>n</i> -triacontane (C ₃₀)	3.27	1.44	4.95	2.01	4.88	1.31	4.67	1.30	4.51	1.61
<i>n</i> -hentriactotane (C ₃₁)	6.47	2.58	8.62	2.70	9.43	2.63	8.42	3.83	8.32	2.97
<i>n</i> -dotriactotane (C ₃₂)	1.51	0.99	2.12	1.27	2.42	0.45	1.74	0.75	1.98	0.94
<i>n</i> -tritriactotane (C ₃₃)	1.73	1.04	2.37	0.78	2.61	0.54	2.16	0.75	2.25	0.79
<i>n</i> -tetraactotane (C ₃₄)	1.09	1.03	1.30	0.69	2.07	0.58	1.06	0.27	1.39	0.75
<i>n</i> -pentactotane (C ₃₅)	1.14	1.10	1.35	0.81	2.69	0.65	1.13	0.23	1.56	0.93
<i>n</i> -alkanes	72.18	22.76	109.76	47.97	110.33	41.29	114.43	44.30	103.21	41.92

The patterns of the *n*-alkanes as a function of the carbon number showed some similarities among the four seasons (Figure 4). The average concentrations in the four

seasons (summer, autumn, winter, and spring) were 72.18, 109.76, 110.33, and 114.43 ng/m³, respectively (Table 2). The lowest value was observed in summer, and the highest one was observed in spring. The *n*-alkane value in spring was slightly higher than the values in autumn and winter. The contributions to the annual sum *n*-alkanes from different seasons were relatively stable and were 18%, 27%, 27%, and 28% in summer, autumn, winter, and spring, respectively.

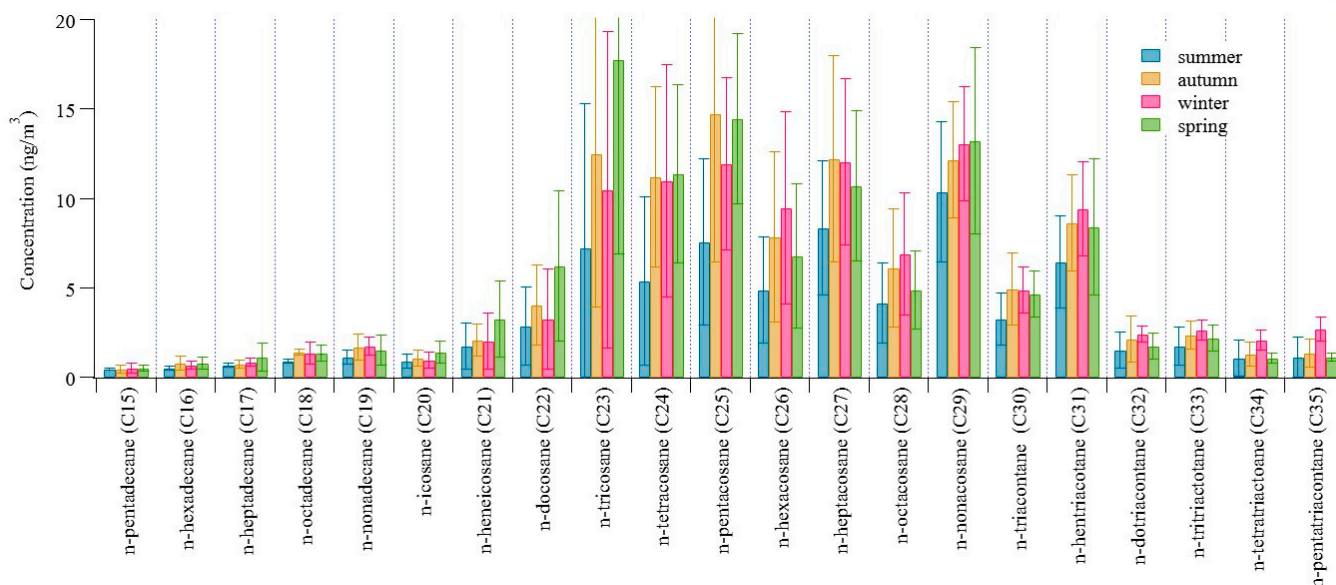


Figure 4. Relative concentration of *n*-alkane species in different seasons (unit: ng/m³; blue: summer, yellow: autumn, red: winter, green: spring).

Aerosol pollution from different sources can be estimated via specific molecular markers of *n*-alkanes. The epicuticular waxes of high plants (angiosperm) are the important contributor to long-chain-length *n*-alkanes (>C₂₄) with a predominance of odd carbon numbers while anthropogenic sources, including fossil fuel burning and vehicular emissions, usually contribute short-chain-length (<C₂₄) *n*-alkanes [11,41,42]. C_{max}, the carbon number exhibiting the highest concentration, is usually used to distinguish biogenic from anthropogenic sources. In this study, C_{max} in summer, autumn, winter, and spring was C₂₉, C₂₅, C₂₉, and C₂₃, respectively. They were characterized by a predominance of odd carbon numbers in the range of C₂₃ to C₂₉. In summer, autumn, and winter, C_{max} of C₂₅ and C₂₉ suggested that biogenic sources contributed greatly to organic aerosol loading. Thus, it is interesting that in spring, the highest *n*-alkane concentration was observed, and C₂₃ was the predominant species, which may be attributed to anthropogenic activities (Rogge et al., 1993; Hong et al., 2017). However, our previous study reported that the air masses that reached TC are relatively clean, with low PM_{2.5} concentrations, during spring [19], indicating that the observed C₂₃ is not predominantly from the anthropogenic source. With the warm temperatures (~26 °C) and high relative humidity (~86%) in spring, the growth of moss, an important source of C₂₃ [43], is likely in favor. The sampling site is surrounded by high mountains, which may be embedded with a considerable amount of C₂₃ emission sources. The predominant *n*-alkane species in the other three seasons also supports the idea that the dominant source at this site was biogenic emission.

3.3. Source Identification of PAHs and *n*-Alkanes

3.3.1. Diagnostic Ratios of PAHs and Their Relations with Gases and Major Water-Soluble Ions

Diagnostic ratios were used to identify the possible sources of PAHs. Tobiszewski and Namieśnik [8] summarized the PAH diagnostic ratios for the identification of pollutant emissions in different environmental compartments, e.g., ratios of Ant/(Phe + Ant),

Flu/(Flu + Pyr), IcdP/(IcdP + BghiP), and BaA/(BaA + Chr). However, the ratio of BaA/(BaA + Chr) is sensitive to atmospheric photoreaction, and it is still difficult to differentiate diesel emissions and biomass burning from the ratio of IcdP/(IcdP + BghiP). Therefore, in this study, we only provide a simple estimation by using the ratios of Ant/(Phe + Ant) and Flu/(Flu+Pyr) to distinguish the possible categories of PAH sources in the environment. It has been reported that a ratio of Ant/(Ant + Phe) higher than 0.1 can be used as an indicator of a combustion source [8]. The Ant/(Ant + Phe) ratio in this study ranged from 0.24 to 0.59, with average values of 0.38 in summer, 0.43 in autumn, 0.33 in winter, and 0.41 in spring. The ratios in different seasons were higher than 0.1, suggesting that combustion sources of PAHs were dominant at the TC site. A diagnostic ratio of Flu/(Flu + Pyr) lower than 0.4, between 0.4 and 0.5, and higher than 0.5 indicates petroleum, fossil fuel combustion, and grass, wood, and coal combustion, respectively [8,25]. There was no difference in the average Flu/(Flu + Pyr) ratios in the four seasons, which were 0.67, 0.65, 0.65, and 0.67 in summer, autumn, winter, and spring, respectively. Therefore, grass, wood, and coal combustion was suggested to be the dominant source at the sampling site.

Moderate correlations between PAHs and sulfate ($R^2 = 0.60$) and SO_2 ($R^2 = 0.77$) were observed in summer and spring. In autumn and winter, PAHs were moderately correlated with potassium ($R^2 = 0.69$), which supports the conclusion from diagnostic ratios and a previous study [32]. In the Hong Kong suburban area, the dominant sources of PAHs are coal and biomass burning. Very weak correlations between PAHs and NO_x ($R^2 = 0.17$) and CO ($R^2 = 0.18$) were observed, indicating that the contribution from local traffic was limited. A moderate correlation ($R^2 = 0.55$) between O_3 and PAHs was found in summer and spring, and no correlation ($R^2 = 0.01$) between the two species was observed in autumn and spring.

3.3.2. Carbon Preference Index (CPI) and Contribution of Plant Wax

The carbon preference index (CPI) is used to investigate the relative contributions of biogenic and anthropogenic emissions and is defined as the ratio of the total odd number of n -alkanes to the even number of n -alkanes [9,10,25,40,44]. When the CPI value is close to 1, n -alkanes mainly originate from vehicular and fossil fuels while n -alkane emissions are derived from high plants. Terrestrial vegetation usually has a high CPI value (>1). The contribution of biogenic sources increases with increasing CPI values. The equation of the CPI calculation is as follows:

For all n -alkanes measured: $CPI = \sum(C_{17} - C_{39}) / \sum(C_{16} - C_{40})$.

For anthropogenic n -alkanes: $CPI_1 = \sum(C_{17} - C_{25}) / \sum(C_{16} - C_{24})$.

For biogenic n -alkanes: $CPI_2 = \sum(C_{27} - C_{39}) / \sum(C_{26} - C_{38})$.

The CPI value at TC ranged from 1.35 to 2.29, with a mean of 1.74 (Table 3). The highest CPI value was found in spring (1.87), indicating impacts from many biogenic activities, i.e., leaf changes, fungi and pollen dispersal, and blooming during the growing season. A comparable CPI value was observed in summer (1.80), implying that high temperatures favored the evaporation of semivolatile compounds from epicuticular waxes of high plants (angiosperm). CPI_1 ranged from 1.60 to 1.83, with a mean value of 1.72. CPI_2 ranged from 1.58 to 1.94, with a mean value of 1.79. CPI_1 and CPI_2 showed relatively high values, suggesting emissions from plant waxes. This further supports the previous conclusion that a significant impact from biogenic sources occurred at the site during the whole sampling period.

The concentrations of wax n -alkanes (%wax C_n) were used to estimate the relative contributions of biogenic sources versus anthropogenic sources [45]. The %wax C_n was calculated by the following equation:

$$\%waxC_n = \frac{\sum(C_n - 0.5(C_{n-1} + C_{n+1}))}{\sum C_n} \times 100\%$$

where C_n is the concentration of plant wax alkanes, and a negative value of $[C_n - 0.5(C_{n-1} + C_{n+1})]$ is taken as zero. In general, the %wax C_n value is below 20% in an urban area with dominant

vehicular emission [13,46] and a higher %waxC_n value implies a greater contribution from plants or biogenic sources.

Table 3. CPI and %wax values of PM_{2.5}-bound alkanes at TC.

	Summer	Autumn	Winter	Spring	Annual
CPI	1.80 (1.52–2.15)	1.71 (1.50–1.98)	1.58 (1.35–1.82)	1.87 (1.43–2.29)	1.74 (1.35–2.29)
CPI ₁	1.78 (1.30–2.10)	1.68 (1.44–2.22)	1.60 (1.49–1.77)	1.83 (1.70–1.98)	1.72 (1.30–2.22)
CPI ₂	1.94 (1.51–2.64)	1.76 (1.35–2.24)	1.58 (1.25–1.88)	1.92 (1.08–2.60)	1.79 (1.08–2.64)
%wax	45% (34–54%)	43% (34–51%)	37% (28–47%)	47% (31–59%)	43% (28–59%)

The annual average %waxC_n was 43%, with a range of 28% to 59% (Table 3). The value was higher than that in many urban cities, i.e., Ningbo (35%), Guangzhou (17%), and Beijing (20%), indicating that %waxC_n in the incomplete combustion of fossil fuels and petroleum residue and municipal incineration was 17% and 25%, respectively [13,15,40]. In our study, %waxC_n in the four seasons was higher than 30%, indicating that epicuticular wax and biogenic sources might play a more prominent role in the large abundance of *n*-alkanes in this area.

4. Conclusions

In this study, PM_{2.5} samples were collected in four nonconsecutive months, August, November, February, and May, in 2011–2012, representing summer, autumn, winter, and spring, respectively. The samples were used to investigate the characteristics of PAHs and *n*-alkanes, including their concentration, seasonal variation, and potential sources in the Hong Kong suburban area, TC. In addition, the health risk for PAHs exposure was also assessed. The annual average concentration of particulate PAHs was 2.57 ng/m³, ranging from 1.26–13.93 ng/m³. The most abundant species were Phe and Flu, which constituted 13% and 18%, respectively. The 4-ring species were dominant in summer, winter, and spring, accounting for over 40%. In autumn, the 5,6,7-ring species contributed the most, ~45%. By comparing the BaP and BaP_{eq} values with ambient air quality standards and the reported values in worldwide cities, the values in our study are much lower, suggesting that PAH pollution at the TC site is not serious. The ILCR value in our study exceeded 1×10^{-6} but was below 1×10^{-4} , implying that the inhalation cancer risk of PAHs at the TC site is acceptable. However, the presence of oxidants (i.e., O₃ and NO_x) can favor the formation of PAH derivatives and it may have a more toxic effect on human health. Therefore, future study on determining the PAH derivatives at this site is essential. The concentration of *n*-alkane ranged from 35.58 to 191.44 ng/m³. C₂₅ was the most abundant species. For *n*-alkanes, a lower value was found in summer, but the highest value was found in spring. Based on the CPI and %wax values, biogenic sources were the major sources of *n*-alkanes at the sampling site. The annual average contribution of higher plant wax to *n*-alkane was up to 40%. PAHs were mainly emitted from coal and biomass burning based on the results, diagnostic ratios, and correlations with source indicators.

Our results reveal the characteristics of PAHs and *n*-alkanes in a Hong Kong suburban site, which can provide a useful reference for future study to evaluate the characteristics of PAHs and *n*-alkanes in the different microenvironments of Hong Kong.

Supplementary Materials: The following supporting information can be downloaded at: <https://www.mdpi.com/article/10.3390/atmos13060980/s1>, Figure S1: correlation plot between (a) PAH and sulfate, SO₂ in summer and spring seasons; (b) PAH and potassium, O₃ in autumn and winter seasons; (c) PAH and NO_x, CO in whole sampling period.; Table S1: Meteorological data during the whole sampling period; Table S2: Data of PM_{2.5}, potassium, sulfate, chloride, nitrate, sodium, calcium, ammonium, NO_x, SO₂, O₃ and CO during the whole sampling period.

Author Contributions: Data analysis, writing—original draft, visualization, Y.G.; review and editing, supervision, Z.L.; data curation, investigation, Z.Z.; review and editing, supervision, project administration, S.L. All authors have read and agreed to the published version of the manuscript.

Funding: The research was supported by Research Start-up fund of Beijing Normal University at Zhuhai (28714-111032101) and Environmental Conservation Fund of Hong Kong (7/2009).

Institutional Review Board Statement: Not applicable.

Informed Consent Statement: Not applicable.

Data Availability Statement: Not applicable.

Conflicts of Interest: The authors declare no conflict of interest.

References

1. Vega, E.; Reyes, E.; Ruiz, H.; García, J.; Sánchez, G.; Martínez-Villa, G.; González, U.; Chow, J.C.; Watson, J.G. Analysis of PM_{2.5} and PM₁₀ in the Atmosphere of Mexico City during 2000–2002. *J. Air Waste Manag. Assoc.* **2004**, *54*, 786–798. [[CrossRef](#)] [[PubMed](#)]
2. Venkataraman, C.; Reddy, C.K.; Josson, S.; Reddy, M.S. Aerosol size and chemical characteristics at Mumbai, India, during the INDOEX-1999. *Atmos. Environ.* **2002**, *36*, 1979–1991. [[CrossRef](#)]
3. Wu, X.; Vu, T.V.; Shi, Z.; Harrison, R.M.; Liu, D.; Cen, K. Characterization and source apportionment of carbonaceous PM_{2.5} particles in China—A review. *Atmos. Environ.* **2018**, *189*, 187–212. [[CrossRef](#)]
4. Joseph, A.E.; Unnikrishnan, S.; Kumar, R. Chemical characterization and mass closure of fine aerosol for different land use patterns in Mumbai city. *Aerosol Air Qual. Res.* **2012**, *12*, 61–72. [[CrossRef](#)]
5. Cao, J.J.; Lee, S.C.; Chow, J.C.; Watson, J.G.; Ho, K.F.; Zhang, R.J.; Jin, Z.D.; Shen, Z.X.; Chen, G.C.; Kang, Y.M.; et al. Spatial and seasonal distributions of carbonaceous aerosols over China. *J. Geophys. Res.-Atmos.* **2007**, *112*, D22. [[CrossRef](#)]
6. Kalberer, M.; Sax, M.; Samburova, V. Molecular Size Evolution of Oligomers in Organic Aerosols Collected in Urban Atmospheres and Generated in a Smog Chamber. *Environ. Sci. Technol.* **2006**, *40*, 5917–5922. [[CrossRef](#)]
7. Ravindra, K.; Sokhi, R.; Van Grieken, R. Atmospheric polycyclic aromatic hydrocarbons: Source attribution, emission factors and regulation. *Atmos. Environ.* **2008**, *42*, 2895–2921. [[CrossRef](#)]
8. Tobiszewski, M.; Namieśnik, J. PAH diagnostic ratios for the identification of pollution emission sources. *Environ. Pollut.* **2012**, *162*, 110–1109. [[CrossRef](#)]
9. Simoneit, B.R.T.; Mazurek, M.A. Organic matter of the troposphere—II. For Part I, see Simoneit et al. (1977). Natural background of biogenic lipid matter in aerosols over the rural western United States. *Atmos. Environ.* (1967) **1982**, *16*, 2139–2159. [[CrossRef](#)]
10. Simoneit, B.R.T. Organic matter of the troposphere—III. Characterization and sources of petroleum and pyrogenic residues in aerosols over the western United States. *Atmos. Environ.* (1967) **1984**, *18*, 51–67. [[CrossRef](#)]
11. Rogge, W.F.; Hildemann, L.M.; Mazurek, M.A.; Cass, G.R.; Simoneit, B.R.T. Sources of fine organic aerosol. 4. Particulate abrasion products from leaf surfaces of urban plants. *Environ. Sci. Technol.* **1993**, *27*, 2700–2711. [[CrossRef](#)]
12. Lammel, G. Polycyclic Aromatic Compounds in the Atmosphere—A Review Identifying Research Needs. *Polycycl. Aromat. Compd.* **2015**, *35*, 316–329. [[CrossRef](#)]
13. Wang, J.; Ho, S.S.H.; Ma, S.; Cao, J.; Dai, W.; Liu, S.; Shen, Z.; Huang, R.; Wang, G.; Han, Y. Characterization of PM_{2.5} in Guangzhou, China: Uses of organic markers for supporting source apportionment. *Sci. Total Environ.* **2016**, *550*, 961–971. [[CrossRef](#)]
14. Wang, G.; Kawamura, K. Molecular Characteristics of Urban Organic Aerosols from Nanjing: A Case Study of a Mega-City in China. *Environ. Sci. Technol.* **2005**, *39*, 7430–7438. [[CrossRef](#)] [[PubMed](#)]
15. Huang, X.-F.; He, L.-Y.; Hu, M.; Zhang, Y.-H. Annual variation of particulate organic compounds in PM_{2.5} in the urban atmosphere of Beijing. *Atmos. Environ.* **2006**, *40*, 2449–2458. [[CrossRef](#)]
16. Chen, Y.; Cao, J.; Zhao, J.; Xu, H.; Arimoto, R.; Wang, G.; Han, Y.; Shen, Z.; Li, G. n-Alkanes and polycyclic aromatic hydrocarbons in total suspended particulates from the southeastern Tibetan Plateau: Concentrations, seasonal variations, and sources. *Sci. Total Environ.* **2014**, *470*, 9–18. [[CrossRef](#)]
17. Guo, H.; Lee, S.C.; Ho, K.F.; Wang, X.M.; Zou, S.C. Particle-associated polycyclic aromatic hydrocarbons in urban air of Hong Kong. *Atmos. Environ.* **2003**, *37*, 5307–5317. [[CrossRef](#)]
18. Ho, K.F.; Lee, S.C. Identification of atmospheric volatile organic compounds (VOCs), polycyclic aromatic hydrocarbons (PAHs) and carbonyl compounds in Hong Kong. *Sci. Total Environ.* **2002**, *289*, 145–158. [[CrossRef](#)]
19. Gao, Y.; Lee, S.-C.; Huang, Y.; Chow, J.C.; Watson, J.G. Chemical characterization and source apportionment of size-resolved particles in Hong Kong sub-urban area. *Atmos. Res.* **2016**, *170*, 112–122. [[CrossRef](#)]
20. Ho, K.F.; Cao, J.J.; Lee, S.C.; Chan, C.K. Source apportionment of PM_{2.5} in urban area of Hong Kong. *J. Hazard. Mater.* **2006**, *138*, 73–85. [[CrossRef](#)]

21. Ho, S.S.H.; Chow, J.C.; Watson, J.G.; Ting Ng, L.P.; Kwok, Y.; Ho, K.F.; Cao, J. Precautions for in-injection port thermal desorption-gas chromatography/mass spectrometry (TD-GC/MS) as applied to aerosol filter samples. *Atmos. Environ.* **2011**, *45*, 1491–1496. [[CrossRef](#)]
22. Nisbet, I.C.T.; LaGoy, P.K. Toxic equivalency factors (TEFs) for polycyclic aromatic hydrocarbons (PAHs). *Regul. Toxicol. Pharmacol.* **1992**, *16*, 290–300. [[CrossRef](#)]
23. Europe, W. Air quality guidelines for Europe. *Eur. Ser.* **2000**, *3*, 23.
24. Gao, Y.; Ji, H. Characteristics of polycyclic aromatic hydrocarbons components in fine particle during heavy polluting phase of each season in urban Beijing. *Chemosphere* **2018**, *212*, 346–357. [[CrossRef](#)] [[PubMed](#)]
25. Zhang, N.; Cao, J.; Li, L.; Ho, S.S.H.; Wang, Q.; Zhu, C.; Wang, L. Characteristics and Source Identification of Polycyclic Aromatic Hydrocarbons and n-Alkanes in PM_{2.5} in Xiamen. *Aerosol Air Qual. Res.* **2018**, *18*, 1673–1683. [[CrossRef](#)]
26. Li, J.; Zhang, G.; Li, X.D.; Qi, S.H.; Liu, G.Q.; Peng, X.Z. Source seasonality of polycyclic aromatic hydrocarbons (PAHs) in a subtropical city, Guangzhou, South China. *Sci. Total Environ.* **2006**, *355*, 145–155. [[CrossRef](#)]
27. Wang, J.; Ho, S.S.H.; Cao, J.; Huang, R.; Zhou, J.; Zhao, Y.; Xu, H.; Liu, S.; Wang, G.; Shen, Z.; et al. Characteristics and major sources of carbonaceous aerosols in PM_{2.5} from Sanya, China. *Sci. Total Environ.* **2015**, *530*, 110–119. [[CrossRef](#)]
28. Liu, F.; Xu, Y.; Liu, J.; Liu, D.; Li, J.; Zhang, G.; Li, X.; Zou, S.; Lai, S. Atmospheric deposition of polycyclic aromatic hydrocarbons (PAHs) to a coastal site of Hong Kong, South China. *Atmos. Environ.* **2013**, *69*, 265–272. [[CrossRef](#)]
29. Moon, K.J.; Han, J.S.; Ghim, Y.S.; Kim, Y.J. Source apportionment of fine carbonaceous particles by positive matrix factorization at Gosan background site in East Asia. *Environ. Int.* **2008**, *34*, 654–664. [[CrossRef](#)]
30. Vestenius, M.; Leppänen, S.; Anttila, P.; Kyllönen, K.; Hatakka, J.; Hellén, H.; Hyvärinen, A.-P.; Hakola, H. Background concentrations and source apportionment of polycyclic aromatic hydrocarbons in south-eastern Finland. *Atmos. Environ.* **2011**, *45*, 3391–3399. [[CrossRef](#)]
31. Zheng, M.; Fang, M. Particle-associated Polycyclic Aromatic Hydrocarbons in the Atmosphere of Hong Kong. *Water Air Soil Pollut.* **2000**, *117*, 175–189. [[CrossRef](#)]
32. Ma, Y.; Cheng, Y.; Qiu, X.; Lin, Y.; Cao, J.; Hu, D. A quantitative assessment of source contributions to fine particulate matter (PM_{2.5})-bound polycyclic aromatic hydrocarbons (PAHs) and their nitrated and hydroxylated derivatives in Hong Kong. *Environ. Pollut.* **2016**, *219*, 742–749. [[CrossRef](#)] [[PubMed](#)]
33. Fan, Z.-L.; Chen, X.-C.; Lui, K.-H.; Ho, S.S.-H.; Cao, J.-J.; Lee, S.-C.; Huang, H.; Ho, K.-F. Relationships between Outdoor and Personal Exposure of Carbonaceous Species and Polycyclic Aromatic Hydrocarbons (PAHs) in Fine Particulate Matter (PM_{2.5}) at Hong Kong. *Aerosol Air Qual. Res.* **2017**, *17*, 666–679. [[CrossRef](#)]
34. Liao, K.; Yu, J.Z. Abundance and sources of benzo[a]pyrene and other PAHs in ambient air in Hong Kong: A review of 20-year measurements (1997–2016). *Chemosphere* **2020**, *259*, 127518. [[CrossRef](#)]
35. Yang, J.; Xu, W.; Cheng, H. Seasonal variations and sources of airborne polycyclic aromatic hydrocarbons (PAHs) in Chengdu, China. *Atmosphere* **2018**, *9*, 63. [[CrossRef](#)]
36. Zhou, S.; Wang, T.; Wang, Z.; Li, W.; Xu, Z.; Wang, X.; Yuan, C.; Poon, C.N.; Louie, P.K.K.; Luk, C.W.Y.; et al. Photochemical evolution of organic aerosols observed in urban plumes from Hong Kong and the Pearl River Delta of China. *Atmos. Environ.* **2014**, *88*, 219–229. [[CrossRef](#)]
37. Ohura, T.; Amagai, T.; Fusaya, M.; Matsushita, H. Spatial Distributions and Profiles of Atmospheric Polycyclic Aromatic Hydrocarbons in Two Industrial Cities in Japan. *Environ. Sci. Technol.* **2004**, *38*, 49–55. [[CrossRef](#)]
38. Smith, D.; Harrison, R.M. Concentrations, trends and vehicle source profile of polynuclear aromatic hydrocarbons in the UK atmosphere. *Atmos. Environ.* **1996**, *30*, 2513–2525. [[CrossRef](#)]
39. Liu, J.; Wang, Y.; Li, P.-H.; Shou, Y.-P.; Li, T.; Yang, M.-M.; Wang, L.; Yue, J.-J.; Yi, X.-L.; Guo, L.-Q. Polycyclic aromatic hydrocarbons (PAHs) at high mountain site in North China: Concentration, source and health risk assessment. *Aerosol Air Qual. Res.* **2017**, *17*, 2867–2877. [[CrossRef](#)]
40. Hong, Z.; Hong, Y.; Zhang, H.; Chen, J.; Xu, L.; Deng, J.; Du, W.; Zhang, Y.; Xiao, H. Pollution Characteristics and Source Apportionment of PM_{2.5}-Bound n-Alkanes in the Yangtze River Delta, China. *Aerosol Air Qual. Res.* **2017**, *17*, 1985–1998. [[CrossRef](#)]
41. Simoneit, B.R.T. Biomass burning—A review of organic tracers for smoke from incomplete combustion. *Appl. Geochem.* **2002**, *17*, 129–162. [[CrossRef](#)]
42. Simoneit, B.R.T. A review of biomarker compounds as source indicators and tracers for air pollution. *Environ. Sci. Pollut. Res.* **1999**, *6*, 159–169. [[CrossRef](#)] [[PubMed](#)]
43. Bush, R.T.; McInerney, F.A. Leaf wax n-alkane distributions in and across modern plants: Implications for paleoecology and chemotaxonomy. *Geochim. Cosmochim. Acta* **2013**, *117*, 161–179. [[CrossRef](#)]
44. Flores, R.M.; Özdemiir, H.; Ünal, A.; Tayanç, M. Distribution and sources of SVOCs in fine and coarse aerosols in the megacity of Istanbul. *Atmos. Res.* **2022**, *271*, 106100. [[CrossRef](#)]
45. Kavouras, I.G.; Lawrence, J.; Koutrakis, P.; Stephanou, E.G.; Oyola, P. Measurement of particulate aliphatic and polynuclear aromatic hydrocarbons in Santiago de Chile: Source reconciliation and evaluation of sampling artifacts. *Atmos. Environ.* **1999**, *33*, 4977–4986. [[CrossRef](#)]
46. Ren, L.; Fu, P.; He, Y.; Hou, J.; Chen, J.; Pavuluri, C.M.; Sun, Y.; Wang, Z. Molecular distributions and compound-specific stable carbon isotopic compositions of lipids in wintertime aerosols from Beijing. *Sci. Rep.* **2016**, *6*, 27481. [[CrossRef](#)]